

cmcR: Congruent Matching Cells Method in R for Cartridge Case Identification

by Joseph Zemmels, Heike Hofmann, Susan VanderPlas

Abstract Firearm evidence identification is the process of analyzing bullets or cartridge cases left at a crime scene to determine if they originated from a particular firearm. Statistical methods have long been developed and used to aid in such analyses. The Congruent Matching Cells (CMC) method is one such method developed at the National Institute of Standards and Technology (NIST) to quantify the similarity between two spent cartridge cases based on the markings left by the firearm barrel during the firing process. We introduce the first open-source implementation of the CMC method in the R package **cmcR**. The package will bolster forensic researchers' abilities to investigate, validate, and improve upon current statistical methodology in the field of forensic science.

Introduction

A *cartridge case* is a type of firearm ammunition that contains a projectile (e.g., bullet, shots, or slug). When a firearm is discharged, the projectile stored in the cartridge case is propelled down the barrel of the firearm. In response, the rest of the cartridge case that remains inside of the firearm is forced towards the back of the barrel. The force with which the cartridge case is propelled backwards causes it to strike the back wall, known as the *breech face*, of the barrel. Markings due to, e.g., manufacturing imperfections are ingrained on the breech face. When the cartridge case slams against the breech face, these markings can be "stamped" into either the primer of the cartridge case or the cartridge case itself. The markings left on a cartridge case from the firearm's breech face are called *breech face impressions*.

An example of two cartridge cases under a comparison microscope is shown in Figure 1 (Michigan State Police, 2020). This type of comparison microscopy involves placing two cartridge cases under separate lenses. The staging areas are combined via a series of lenses, prisms, and mirrors such that both cartridge cases can be seen side by side through a single field of view. A thin, black line can be seen down the center of Figure 1 dividing the view of the two cartridge cases. Similar breech face impression striae are seen on both cartridge cases providing evidence that the pair is a match. Such *individual characteristics* are used by forensic practitioners to declare a cartridge case pair a match (Thompson, 2017).

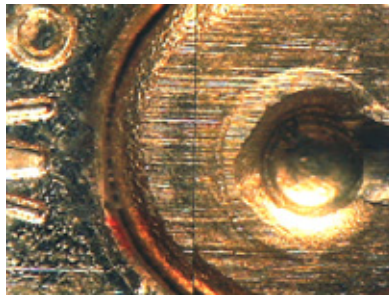


Figure 1: View of two cartridge cases under a comparison microscope

These breech face impressions are considered to be analogous to a firearm's "fingerprint" left on a cartridge case. Matching an expended cartridge case of unknown source to one of known source based on breech face impressions has been performed for over 100 years by forensic practitioners (Thompson, 2017). The development of computational and statistical methods to perform such identification has recently grown in interest (National Research Council, 2009).

One such method is the Congruent Matching Cells (CMC) method developed at NIST that involves partitioning a cartridge case image or scan into a grid of "correlation cells" to isolate areas containing identifying breech face impression markings (Song, 2013). Since its invention in 2012, researchers at NIST have developed a number of extensions and improvements of the CMC method. However, to date there does not exist an openly available implementation of any of these techniques. Many methods proposed in the CMC literature include a description of a proposed technique that do not delve into the intricacies of the implementation. Given that the implementations are not openly available, this makes it especially difficult to validate or assess results. Additionally, some procedures related to pre-processing the cartridge case data are done manually at NIST rather than with an automated method (Song et al., 2018). This compounds the difficulty to accurately reproduce results.

The **cmcR** package provides an open-source, fully-automatic implementation of the CMC method as originally described as well as an extension proposed by [Tong et al. \(2015\)](#). This extension was later referred to as the “High CMC” method by [Chen et al. \(2017\)](#) and is referred to as such in the **cmcR** package.

Cartridge case surface data

Cartridge case data commonly come in two forms: 2D grayscale images and 3D topographical scans. It is common in the CMC literature to use the 3D topographical scans to demonstrate the efficacy of a proposed method [[Tong et al., 2015](#)], ([Chen et al., 2017](#))]. A variety of scans are openly available for download through the NIST Ballistics Toolmark Research Database ([Zheng et al., 2016](#)). The **cmcR** package was designed specifically for use with the 3D topographies.

The 3D topographies are commonly stored in an .x3p (XML 3D Surface Profile) file format that includes metainformation such as who took the scan and the parameters under which the scan was taken (e.g., the lateral resolution in microns). The **x3ptools** package in R provides an interface to manipulate and visualize these .x3p files ([Hofmann et al., 2019](#)). The physical surface is represented using a *surface matrix*: a matrix of spatially-ordered elements or “pixels” whose values correspond to the height of the cartridge case surface at a particular location. Figure 2 shows the surface matrices of a known match (KM) pair of cartridge cases, meaning there were fired from the same firearm. Note that white regions in the images below represent unobserved or missing values. When read into R using the **x3ptools** package, these elements are encoded as NA. The size of a surface matrix depends on the lateral resolution with which the scans were taken. For example, a popular set of scans in the CMC literature were taken by [Fadul et al. \(2011\)](#); two of which are shown in Figure 2. These scans were taken with a lateral resolution of 6.25 microns (micrometers) per pixel. The surface matrices from this study vary around 1200×1200 pixels in size.

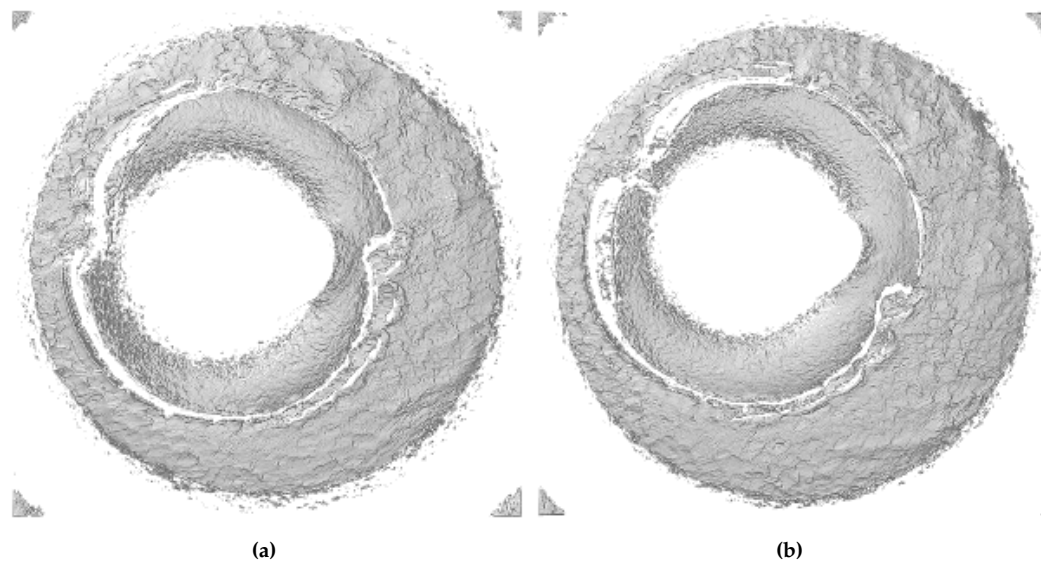


Figure 2: Two known match cartridge case scans from [Fadul et al. \(2011\)](#)

Only certain regions of a cartridge case contain identifying breech face impression markings. [Song \(2013\)](#) refers to these as “valid correlation regions” that are to be used to determine whether two cartridge cases match. The cell-based comparison procedure described in section 3.1 is designed to allow such regions to stand out against invalid correlation regions. However, prior to applying this procedure cartridge scans must undergo some pre-processing to remove sections of the cartridge case surface that do not come into contact with the breech face of the barrel. These include a circular plateaued region in the center of the scan that is pushed aside by the firing pin during the firing process and clusters of observed values in the corners of the scan that are artifacts of the staging area in which the scan was captured. The task in pre-processing is to automatically remove these unwanted regions from the scan to accentuate unique markings left by the breech face. This is discussed in greater detail in section 3.1.

Cell-based surface matrix comparisons

Cell-based comparison procedure

The Congruent Matching Cells method was developed at the National Institute of Standards and Technology to quantify the similarity between two spent cartridge cases based on their breech face impressions. The CMC method involves dividing a breech face impression scan into a grid of cells and comparing each cell in one scan to a counterpart region in the other scan. This method is motivated by the fact that breech face markings are not uniformly impressed upon the cartridge case during the firing process. As such, only certain sections of the cartridge case have identifiable markings that make it possible to match to a firearm. Calculating a similarity score between the entirety of two cartridge case surfaces might not highlight these identifying regions. Instead, the number of highly similar cell/region pairs between the two scans can be used as a more granular similarity metric.

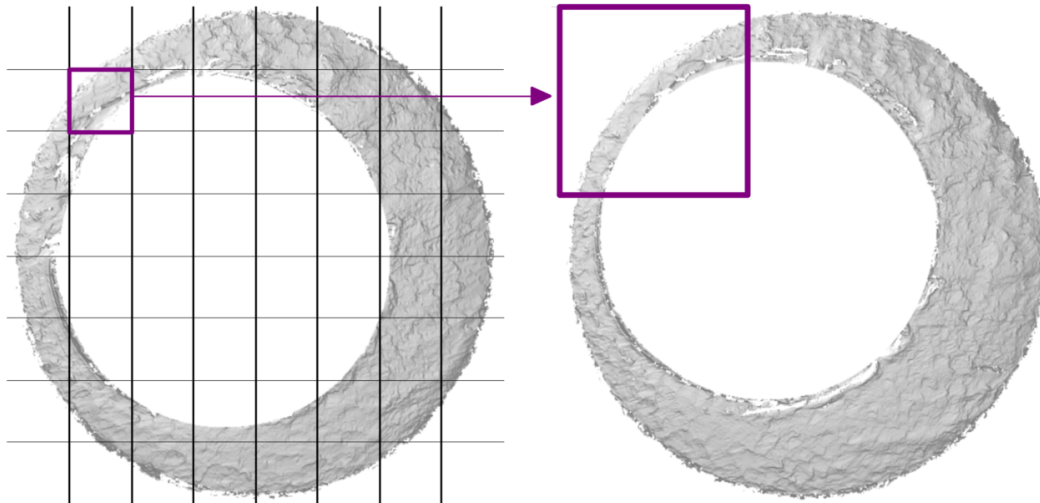


Figure 3: Illustration of comparing a "cell" in one cartridge case scan to a region in another

Figure 3 illustrates the cell-based comparison procedure between two cartridge case scans. The scan on the left is divided into a grid of 8×8 cells. Each cell is paired with an associated larger region in the other scan. The absolute location of each cell and region in their respective surface matrices remain constant. However, the scan on the right is rotated to determine the rotation at which the two scans are the most "similar," which is quantified using the *cross-correlation function* (CCF). For two real-valued, $M \times N$ matrices A and B , the cross-correlation function, denoted $(A \star B)$ can be defined as

$$(A \star B)[m, n] = \sum_{i=0}^M \sum_{j=0}^N A[i, j] B[(i + m)_{\text{mod } M}, (j + n)_{\text{mod } N}].$$

Note that this finite, discretized CCF is a matrix of elements representing the similarity between matrices A and B for various translations of matrix B . The index at which the CCF attains a maximum represents the translations needed to align B with A . When working with cell/region pairs, calculating the CCF from the definition is computationally intractable. The *Cross-Correlation Theorem* provides a feasible alternative to calculating the CCF. For two matrices A and B , the Cross-Correlation Theorem implies that

$$(A \star B)[m, n] = \mathcal{F}^{-1} \left(\overline{\mathcal{F}(A)} \cdot \mathcal{F}(B) \right) [m, n]$$

where \mathcal{F} and \mathcal{F}^{-1} denote the discrete Fourier and inverse discrete Fourier transforms, respectively (Brigham, 1988). Note that the multiplication on the right-hand side is pointwise (Hadamard) multiplication. This result allows us to trade the moving sum computations from the definition of the CCF for two forward Fourier transformation, a pointwise product, and an inverse Fourier transformation. The Fast Fourier Transform (FFT) algorithm is used to reduce the computational load considerably. However, a practical consideration for applying this method with cartridge case data is the large number of non-random missing values in a surface matrix. Recall that missing values are represented in Figures 2 and 3 as white pixels. The discrete Fourier transform is not defined for matrices containing missing values, so these need to be replaced. The convention adopted in the **cmcR** package is to replace missing values with 0 after standardizing a matrix by subtracting away its average height value and dividing by its standard deviation. Such standardization is commonly performed by authors at NIST (Ott et al., 2017). While replacing missing values is essential for using the FFT-based method of

calculating the CCF, doing so causes the CCF values to be “deflated” relative to the *pairwise-complete correlation* in which only pairs of pixels in which neither element is missing are considered. However, the translation estimates obtained from this method are often good estimates for the true translation values by which the two matrices align.

Figure 4 provides an example of the output from the FFT-based CCF calculation method. In the top-left we see a 72×72 pixel cell from one surface matrix. In the top-right we see this cell’s associated region in the other surface matrix of dimension 216×216 (triple the cell’s side lengths). The bottom-left shows the CCF “map” calculated using this FFT-based method. Although the CCF need not be bounded between -1 and 1 based on the definition, it is common to normalize the CCF for interpretability purposes and is done so in the **cmcR** package. A summary of the alignment parameters at which the CCF_{\max} occurs is shown in the bottom-right. We can see that the two matrices are best-aligned when the cell is shifted “east” 20 pixels and “north” 9 pixels starting from the center of the region. The $\theta = -18$ indicates that the overall cartridge case scan from which the region (shown in the top-right) was extracted was rotated by -18 degrees for this comparison. The orange square in the top-right plot shows where the cell would be located if the translation were performed.

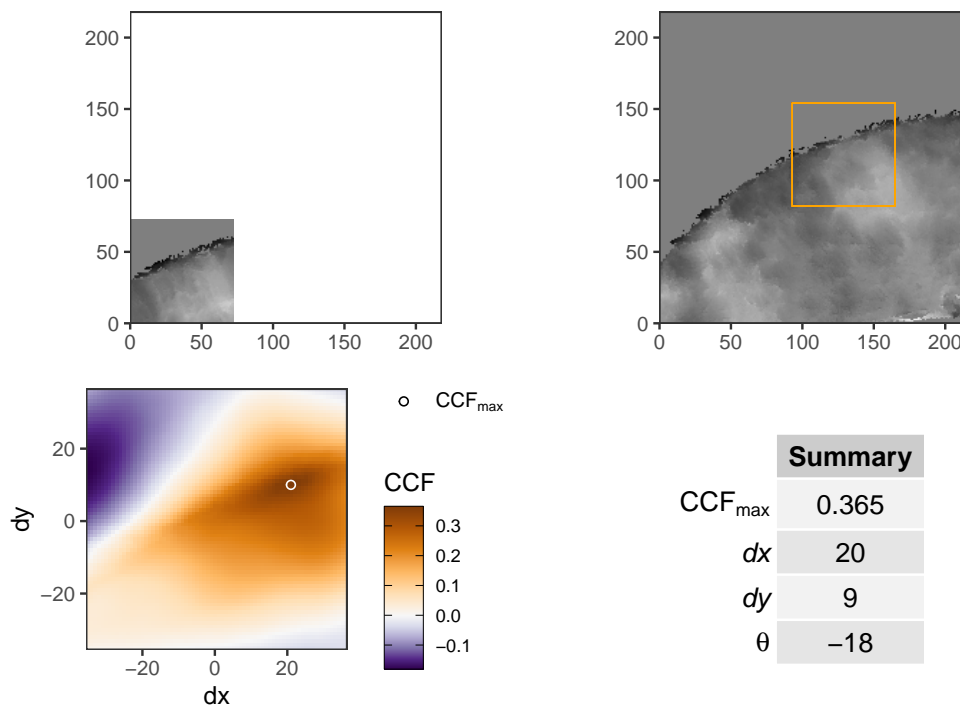


Figure 4: Example of a cross-correlation function “map” for a particular cell/region comparison

Using the estimated translation values at which the CCF_{\max} occurs, we can calculate the pairwise-complete cross-correlation between the cell and a cell-sized matrix extracted from the larger region where missing values are not replaced. Think of this as punching-out the matrix enclosed in the orange square shown in the top-right plot of Figure 4. This will be used as the high CCF_{\max} estimate. This cell-based comparison procedure is performed for each cell/region pair for various rotation values.

The Congruent Matching Cells method

A particular cell/region pair is deemed “highly similar” if it passes a collection of user-defined similarity criteria. The criteria are based on the fact that a pair of matching cartridge case scans are not necessarily aligned properly in their raw format. In particular, one cartridge case scan needs to be rotated and translated to align correctly the other. Let $CCF_{\max}, dx, dy, \theta$ denote the “true” but unknown CCF, translation, and rotation values, respectively, by which a particular pair aligns. These unknown alignment parameters can be estimated for each cell/region pair using the cell-based comparison procedure discussed in section 3.1. Let $CCF_{\max,i}, dx_i, dy_i, \theta_i$ denote the estimated alignment parameter values for cell/region pair $i, i = 1, \dots, n$. For a truly matching pair of cartridge cases, we would expect these alignment parameter estimates to agree with each other across cell/region pairs; at least up to some threshold. Conversely, we would expect the estimates to vary randomly for a truly *non*-matching pair. As such, the CMC method details how to determine whether a consensus exists among the

estimated alignment parameter values across the cell/region pairs. The initially proposed method by Song (2013) as well as an extension by Tong et al. (2015) known as the High CMC method are implemented in the **cmcR** package.

The initially proposed method

The method as originally proposed by Song (2013) considers only the alignment parameter estimates by which each cell/region pair attains its $CCF_{\max,i}$. Intuitively, this can be thought of as only allowing each cell/region pair to “vote” for a single set of alignment parameter values. It’s reasonable to assume that a consensus would exist amongst these values for a truly matching pair of cartridge cases. Song proposes using the median of the dx_i, dy_i, θ_i values as a consensus, although others are certainly plausible. Let $\bar{dx}, \bar{dy}, \bar{\theta}$ denote the consensual alignment parameter values. To declare a particular cell/region pair as “congruent matching,” Song requires that (1) the pair’s estimated alignment parameter values be within some threshold distance of the consensual values and (2) the CCF_{\max} value is greater than some threshold. That is, for thresholds $T_{dx}, T_{dy}, T_{\theta}, T_{CCF}$, cell/region pair i is declared a match if all of the following conditions hold:

1. $|dx_i - \bar{dx}| \leq T_{dx}$
2. $|dy_i - \bar{dy}| \leq T_{dy}$
3. $|\theta_i - \bar{\theta}| \leq T_{\theta}$
4. $CCF_{\max,i} \geq T_{CCF}$.

Song proposes using a minimum of 6 congruent matching cells to declare a cartridge case pair a match, although this threshold is based on a common threshold used in matching bullets via the striae left by a firearm barrel. This has been shown in subsequent extensions to not always be an effective threshold (Chen et al., 2017).

The High CMC method

Experimentation demonstrated that the assumption underlying the initially proposed method, that the $CCF_{\max,i}$ estimated alignment parameter values would reach a consensus across all cell/region pairs, does not always hold in general. In particular, if we only consider the “top” vote for each cell/region pair, then many pairs may vote far away from the consensual value and thus would not be declared congruent matching. However, Tong et al. (2015) observe that such pairs *are* often highly similar at the consensual rotation value, $\bar{\theta}$. The extension they propose utilizes the behavior of the estimated alignment parameter values more advantageously across various rotation values than the initially proposed method. Additionally, comparisons are performed in both “directions” so that each cartridge case scan takes on the role of the scan that is partitioned into a grid of cells.

Tong et al. (2015) propose applying the translation and CCF_{\max} CMC criteria discussed in section 3.2.1 to the comparison results for each rotation value. In doing so, a CMC count for each rotation can be obtained. They identify a common behavior among known match cartridge case pairs that the CMC counts often attain a mode around the rotation value by which they align best. For known non-match pairs, the CMC counts often vary randomly across rotation values. These phenomena are illustrated in Figures 5 and 6. Figure 5 shows the CMC counts per rotation value in both directions for a known match pair of cartridge case scans from Fadul et al. (2011). We can clearly see a CMC mode around $\theta = -21$ in one direction and 21 or 24 in the other, which is to be expected for a known match pair. Figure 6, on the other hand, shows the CMC counts for a known non-match pair. We can see that no such CMC count mode is achieved.

Tong et al. (2015) introduce an additional criterion to identify a mode in the CMC per θ counts. Namely, they introduce a “high” CMC threshold defined to be $CMC_{\text{high}} = CMC_{\max} - \tau$ for some constant τ (they choose $\tau = 1$) where CMC_{\max} is the maximum CMC count attained across all rotation values considered. In the example shown in Figure 5, $CMC_{\max} = 17$ in one direction and 15 in the other. They propose finding the range of rotation values with associated CMC count greater than or equal to CMC_{high} . If this range is greater than the threshold T_{θ} , then there is evidence to suggest that a CMC count mode does not exist and the cartridge case pair is not a match. The CMC_{high} thresholds are shown as horizontal dashed lines in Figures 5 and 6. We can see in Figure 5 that the only θ values with associated CMC counts greater than or equal to CMC_{high} are adjacent. This particular cartridge case pair would “pass” the high CMC criterion. The pair shown in Figure 6 elicit considerably more

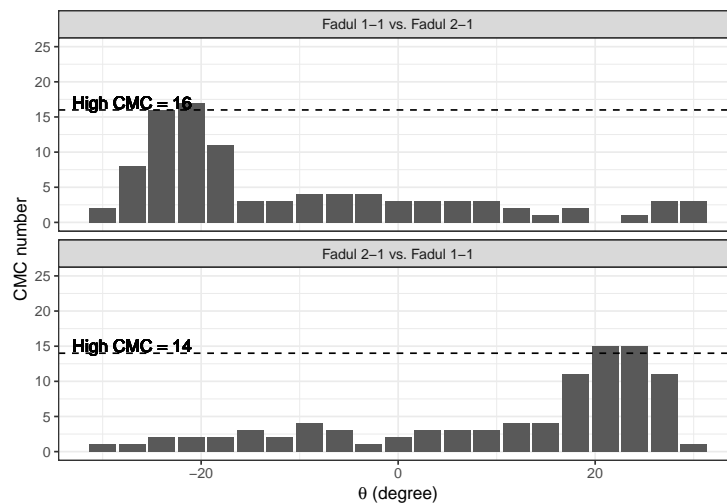


Figure 5: CMC count per rotation (θ) values in both directions for a KM cartridge case pair

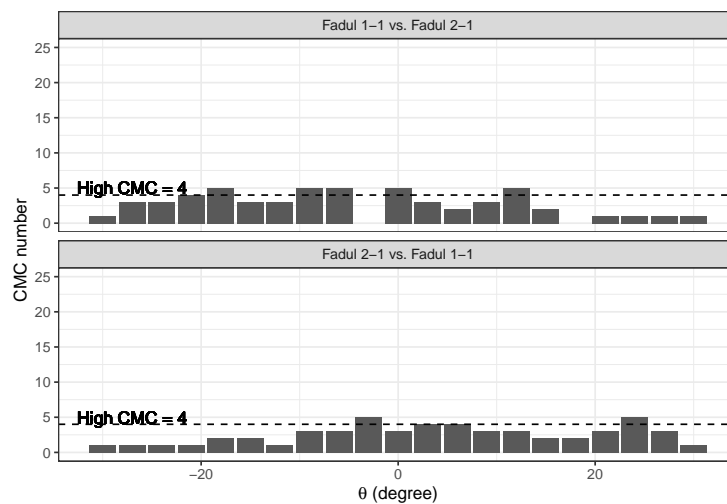


Figure 6: CMC count per rotation (θ) values in both directions for a KNM cartridge case pair

diffuse θ values with associated CMC count great than or equal to CMC_{high} and thus would not pass the high CMC criterion.

Cartridge case pairs that do not pass the high CMC criterion are assigned the CMC count under the initially proposed method. Pairs that pass the criterion are assigned all CMCs in and within T_θ of the identified CMC count mode in both directions (excluding replicate cell/region pairs). Among other considerations, [Tong et al. \(2015\)](#) do not indicate how to deal with adjacent CMC count ties (as is the case in the Fadul 1-2 vs. Fadul 1-1 direction in Figure 5) nor situations in which a CMC count mode is identified in one direction but not the other. This, again, illustrates how a qualitative description of a method often fails to cover critical details. While individually small in scope, leaving such details ambiguous can quickly compound how difficult it is to effectively reproduce results.

The cmcR package

This section will highlight the **cmcR** package's functionality by walking through a possible use case. Many of the functions in this package provide the user with a variety of processing options with which they can experiment. This is due to the fact that processing techniques differ considerably among authors or are not discussed in great detail.

Pre-processing procedures

Studies in which cartridge cases are matched by forensic examiners often involve giving examiners a set of known matches and asking them to classify additional matches from a collection of unknown source scans. For brevity, we will consider a comparison between two cartridge cases from (Fadul et al., 2011). Figure 7 shows the pair of scans after performing the necessary pre-processing procedures. Note that the color scheme has been scaled by quantiles to visually highlight regions of the cartridge case scan containing strong breech face impression “signal.”

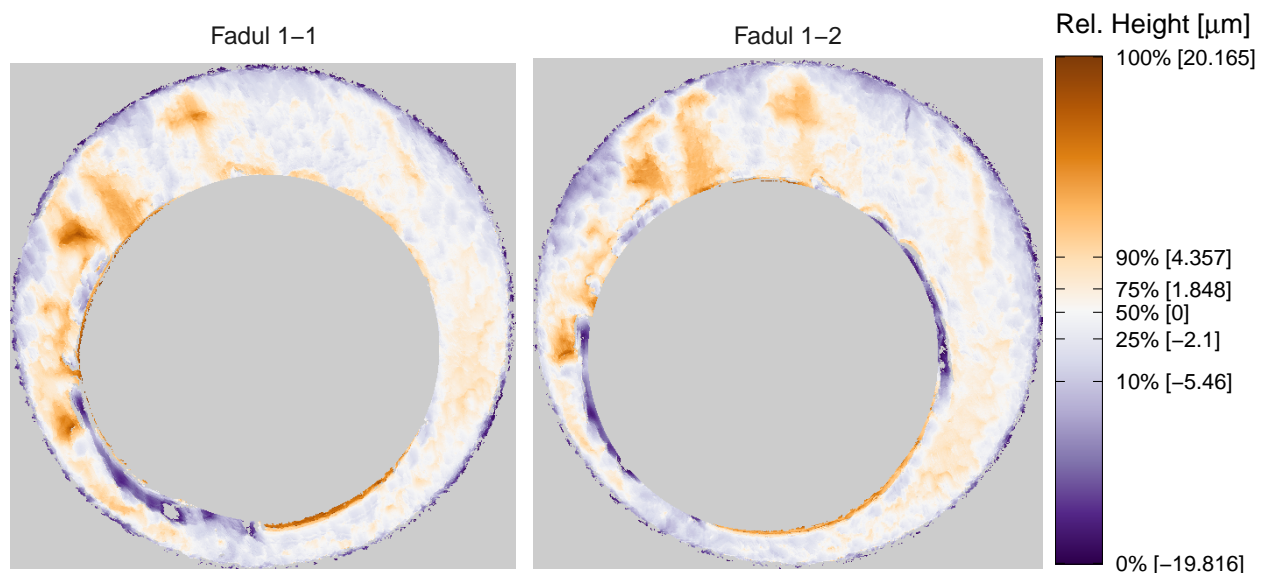


Figure 7: A known match pair of processed cartridge case scans

The family of functions in the **cmcR** package beginning with `preProcess_` can be used to perform the necessary pre-processing steps for a pair of cartridge case scans to be comparable using the cell-based comparison procedure outlined in section 3.1. The implementation of many of these pre-processing procedures is inspired largely by Tai and Eddy (2018) who detail a fully-automatic procedure for processing cartridge case 2D images as opposed to 3D scans. The functions available include:

1. `preProcess_ransac`: estimates the height value of the breech face impressions in a scan using the Random Sample Consensus (RANSAC) robust, iterative plane-fitting algorithm (Fischler and Bolles, 1981).
2. `preProcess_levelBF`: extracts the observations containing breech face impressions from the scan using the estimated height value obtained from `preProcess_levelBF`.
3. `preProcess_cropWS`: removes rows/columns containing mostly if not all NA values from the surface matrix on the exterior of breech face impressions.
4. `preProcess_removeFPCircle`: detects and removes observations within the firing pin impression circle using the Hough Transform circle detection algorithm (Hough, 1962).
5. `preProcess_gaussFilter`: applies a low-pass, high-pass, or band-pass Gaussian filter to the breech face impressions to reduce the effects of high frequency noise, low frequency global structure, or both, respectively.

See the **cmcR** package documentation for more information about these functions.

For computational purposes it is common the CMC literature to down-sample a surface matrix prior to performing the cell-based comparison procedure. The `sample_x3p` function from the **x3ptools** package can be used to sample every m th row/column of a surface matrix. The `selectBFImpression_sample_x3p` performs all of these pre-processing procedures in a single call. The code to produce the first surface matrix shown in Figure 7 is given by the following example. Note that the RANSAC method relies on randomly selecting points within the surface matrix, so a seed is set for reproducibility.

```
library(cmcR)
library(x3ptools)
library(magrittr)
set.seed(4132020)
```

```

nrbtd_url <- "https://tsapps.nist.gov/NRBD/Studies/CartridgeMeasurement/"

fadul1.1_id <- "DownloadMeasurement/2d9cc51f-6f66-40a0-973a-a9292dbec36d"
fadul1.2_id <- "DownloadMeasurement/cb296c98-39f5-46eb-abff-320a2f5568e8"

fadul1.1 <- selectBFImpression_sample_x3p(x3p_path = paste0(nrbtd_url,fadul1.1_id),
  ransacInlierThresh = 1e-5, #1 micron
  ransacIters = 150,
  croppingThresh = 1,
  m = 2, #sample_x3p down-sample rate
  gaussFilterWavelength = c(16,250),
  gaussFilterType = "bp") #band-pass filter

```

Implementation of cell-based comparison procedure

The cell-based comparison procedure outlined in section 3.1 is implemented in the `cellCCF_bothDirections` function. In particular, the procedure is performed twice so that both cartridge case scans take on the role of the scan that is partitioned into a grid of cells. This is necessary to apply the High CMC logic discussed in section 3.2.2. Continuing with the current use case example, the code to perform this procedure on `fadul1.1` and `fadul1.2` is given by the following example.

```

kmComparison <- cellCCF_bothDirections(x3p1 = fadul1.1,
  x3p2 = fadul1.2,
  thetas = seq(-30,30,by = 3),
  cellNumHoriz = 8,
  cellNumVert = cellNumHoriz,
  minObservedProp = .1)

```

The first few rows of results from the comparison between `fadul1.1` and `fadul1.2` in which `fadul1.1` was divided into a grid of cells and `fadul1.2` was rotated by 3 degrees is given below. Although a grid of 8×8 cells were used, there were only 43 cell/region pairs that contained a sufficient proportion of non-missing values (10% in this example). Recall that the features used in the CMC method are the CCF_{\max} values (`ccf` column) and estimated alignment parameter values (`dx`, `dy`, and `theta` columns).

```
head(kmComparison$comparison_1to2$ccfResults$`3`)
```

Table 1: Example of output from `cellCCF` function

| cellNum | cellID | ccf | fft.ccf | dx | dy | theta |
|---------|---------------------------|-----------|-----------|-----|-----|-------|
| 2 | y = 1 - 73, x = 74 - 145 | 0.7762319 | 0.2108462 | 34 | -30 | 3 |
| 3 | y = 1 - 73, x = 146 - 217 | 0.1006877 | 0.1145874 | 29 | 22 | 3 |
| 4 | y = 1 - 73, x = 218 - 289 | 0.1863672 | 0.1030728 | -32 | -16 | 3 |
| 5 | y = 1 - 73, x = 290 - 362 | 0.8004083 | 0.3658809 | 5 | 4 | 3 |
| 6 | y = 1 - 73, x = 363 - 434 | 0.7036884 | 0.2353348 | 22 | 10 | 3 |
| 7 | y = 1 - 73, x = 435 - 506 | 0.7965972 | 0.1407746 | -25 | -18 | 3 |

Congruent Matching Cells logic

The `cmcFilter_improved` function determines both the initial and high CMCs for a particular comparison. The example below shows how to use the function with thresholds defined similar to those in Song et al. (2018).

```

kmCMC <- cmcR::cmcFilter_improved(kmComparison,
  ccf_thresh = .5,
  dx_thresh = 20,
  dy_thresh = 20,
  theta_thresh = 6)

```

The `cmcPlot` function will construct a plot to visualize cells have been declared a CMC and those that have not. The initial 21 CMCs and 22 non-CMCs for the current use case example are shown

in black and red, respectively, on the left-hand side of Figure 8. Black cells on the right-hand side of Figure 8 show how each CMC aligns in the other surface matrix. The red cells show how the non-CMCs align to attain their CCF_{\max} value.

```
cmcPlots <- cmcR::cmcPlot(fadul1.1$x3p,
                          fadul1.2$x3p,
                          cellCCF_bothDirections_output = kmComparison,
                          cmcFilter_improved_output = kmCMC,
                          x3pNames = c("Fadul 1-1", "Fadul 1-2"))
```

```
cmcPlots$initialCMC
```

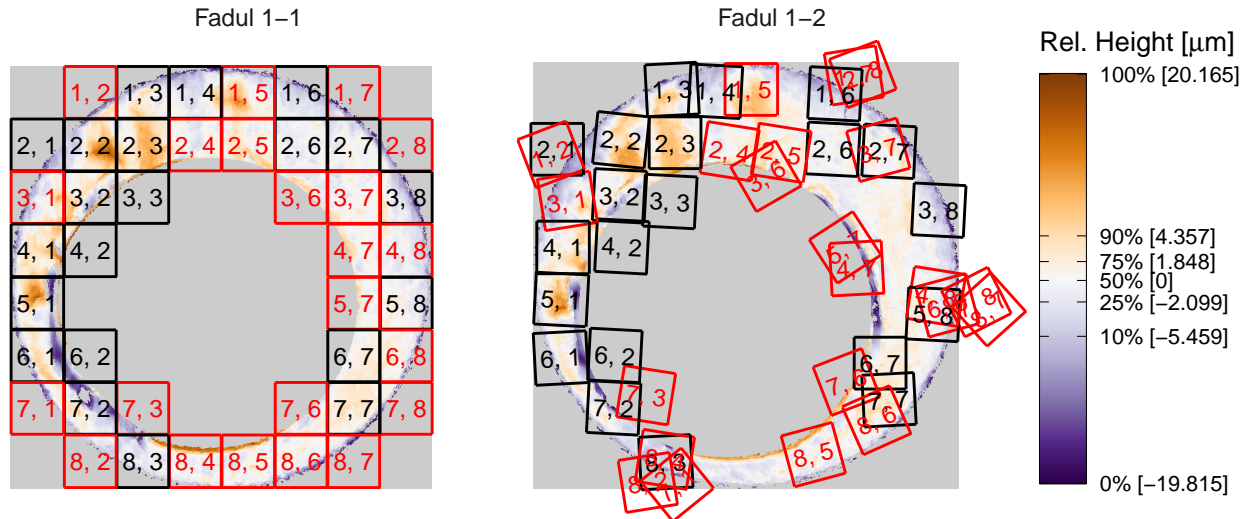


Figure 8: CMC results from a known match comparison under the initially proposed method

Similarly, 41 CMCs and 2 non-CMCs determined under the High CMC method are shown in Figure 9.

```
cmcPlots$highCMC
```

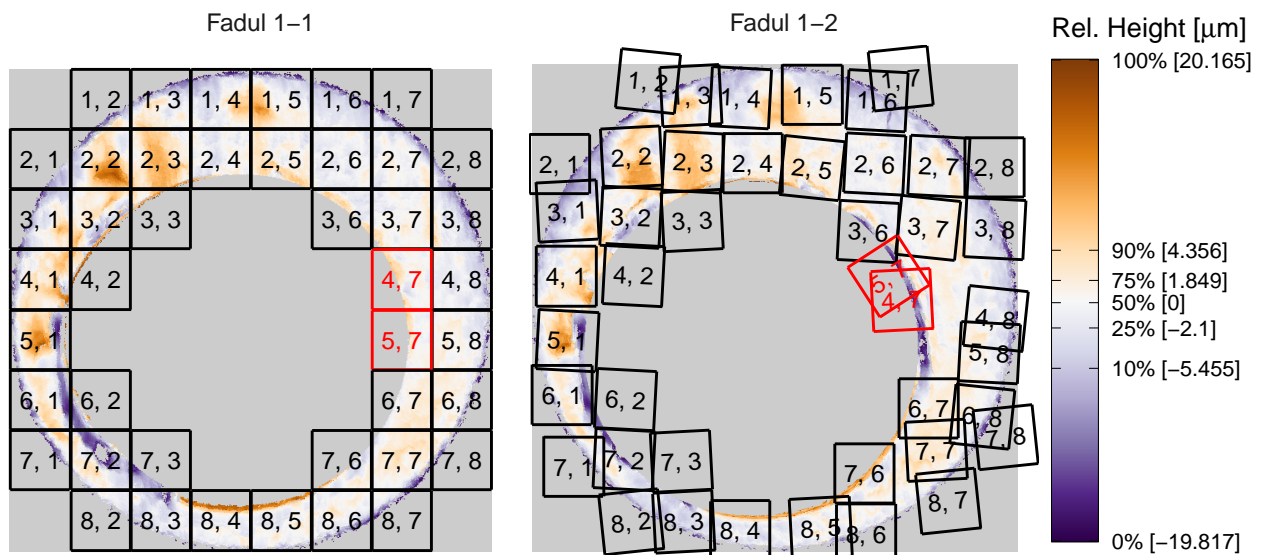


Figure 9: CMC results from a known match comparison under the High CMC method

In contrast, Figure 10 shows the CMC results for a comparison between Fadul 1-1 and a known non-match scan, Fadul 2-1, under the same pre, inter, and post-processing conditions used for the known match comparison. We can see that 6 initial CMCs were determined while there were 0 CMCs under the High CMC method.

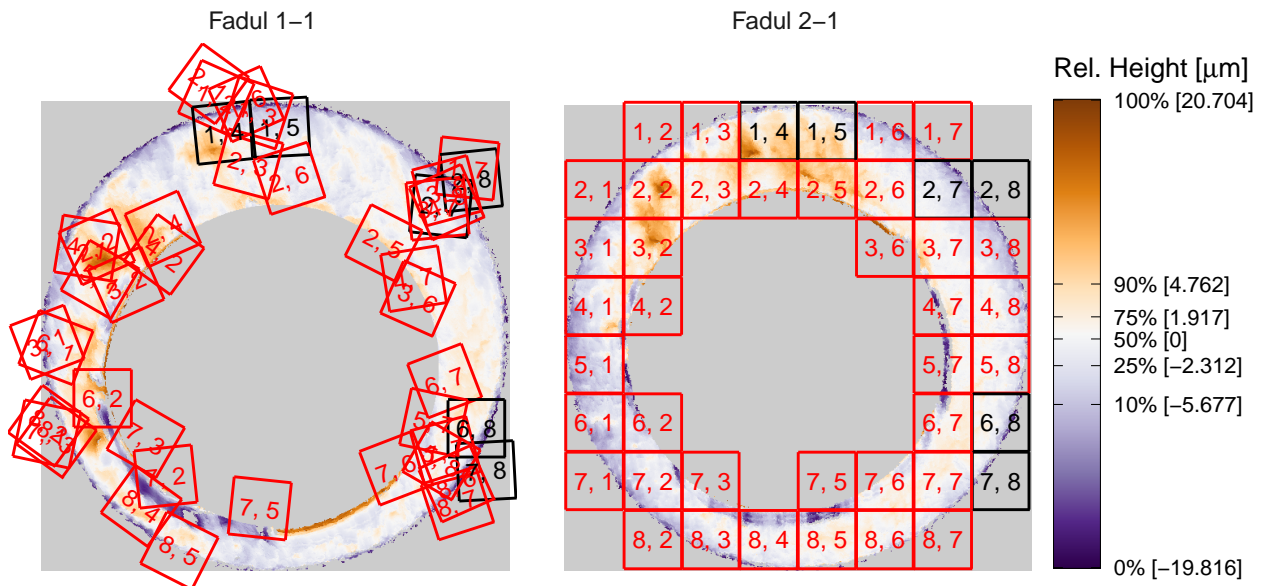


Figure 10: CMC results from a known non-match comparison under the initially proposed method

Results

As described in section 2, the set of cartridge case scans from [Fadul et al. \(2011\)](#) is commonly used to compare the performance of various methods in the CMC literature. This set consists of 40 cartridge cases. There are 63 known match pairs and 717 known non-match pairs. While the exact procedures by which these scans are processed are unavailable, the surface data are openly available in their raw, unprocessed format NIST Ballistics Toolmark Research Database. Thus, some level of comparison between the implementation provided in the **cmcR** package and published results is possible. However, justification for any differences will ultimately involve educated hypothesization due to the closed-source nature of the original implementations.

For any cartridge case pair, the number of CMCs can be determined under the initially proposed method described in section 3.2.1 and the high CMC method described in section 3.2.2. These CMC counts can be determined for all 780 cartridge case pairs available in the [Fadul et al. \(2011\)](#) dataset. Perfect identification of all matching and non-matching pairs corresponds choosing a CMC count threshold that separates the distributions of the matching and non-matching CMC counts. Many authors have found success in choosing a CMC count threshold of 6 CMCs ([Tong et al. \(2015\)](#), [Song et al. \(2018\)](#)) as initially proposed by [Song \(2013\)](#), although this threshold has been shown to not generalize well to all proposed methods or cartridge case datasets ([Chen et al., 2017](#)). Further, little consensus exists among authors on the most effective alignment parameter thresholds (T_{dx} , T_{dy} , T_{θ} , T_{CCF} defined in section 3.2.1) for distinguishing matches from non-matches. Figure 13 shows an example of a particular set of thresholds that yields separation between the known match and known non-match CMC count distributions. An appropriate CMC count threshold would be where the dashed, vertical line is drawn at 15.5 CMCs. Separation is also achieved using the initially proposed method by [Tong et al. \(2015\)](#) and [Chen et al. \(2017\)](#), among others. It should be noted that these authors report CMC count distributions with fewer “false positive” CMCs for non-match pairs. However, the behavior of these distributions changes considerably depending on the thresholds specified.

Figure 12 shows the CMC count distributions determined using the initially proposed method for various CCF and translation thresholds. The rotation threshold was fixed at $T_{\theta} = 3$ degrees. The most restrictive threshold combination is in the bottom left corner while the least restrictive, which is also shown in Figure 13, is in the top right corner. As expected, fewer CMCs are assigned to all pairs as the thresholds become more restrictive. Additionally, many threshold combinations yield overlapping matching and non-matching CMC count distributions making perfect identification based on a minimum CMC count threshold impossible.

Figure 13 shows an example of threshold combinations that yield separation between the matching and non-matching CMC count distributions. The dashed, vertical line is drawn at 35.5 CMCs. Note that while known match pairs tend to be assigned higher CMC counts than under the initially proposed method, so too do certain known non-match pairs. The cluster of non-match pairs that are assigned a

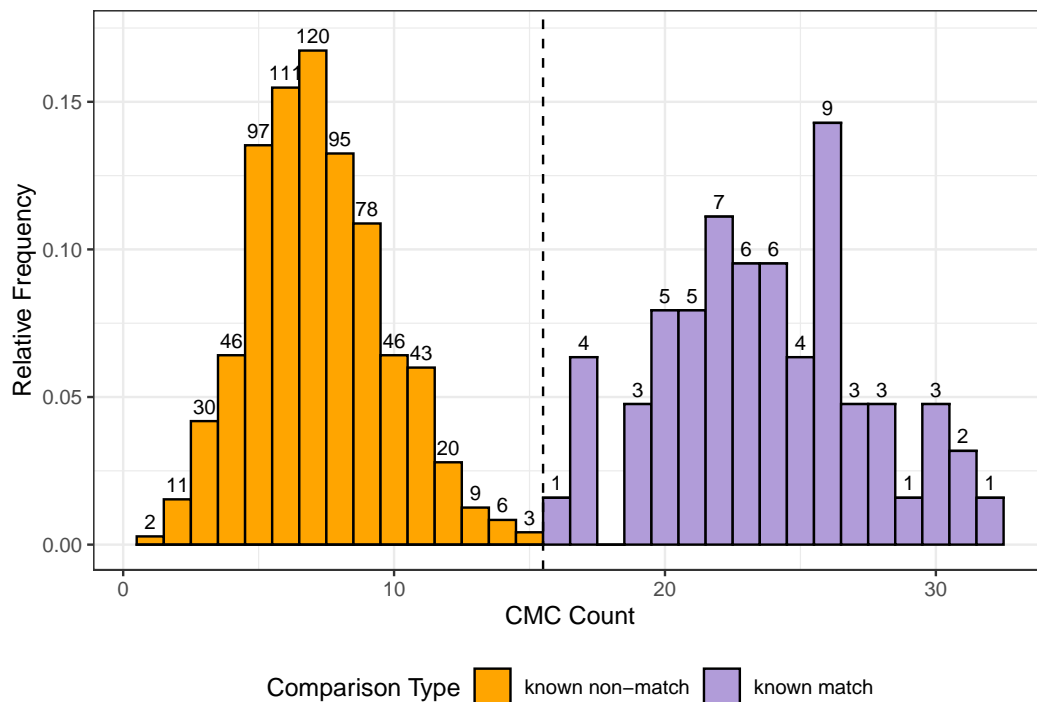


Figure 11: Initial CMC count distribution with $T_{CCF} = .5$, $T_{dx} = T_{dy} = 30$, and $T_{\theta} = 6$ degrees.

large High CMC count all pass the High CMC criterion. Similar non-match bimodal behavior can be seen in Figure 8 of [Chen et al. \(2017\)](#) where the High CMC method was applied to cartridge case data from [La Porte \(2011\)](#).

Figure 14 shows CMC count distributions determined using the High CMC method for various CCF and translation thresholds. Again, there are many threshold combinations that yield a large number of false positive CMCs to non-matches due to the associated pairs passing the High CMC criterion. Conversely, matching pairs assigned relatively small CMC counts are those that do not pass High CMC criterion. This demonstrates that if any cartridge case pair, matching or non-matching, passes the High CMC criterion, then it tends to be assigned a large High CMC count. Tuning the thresholding parameters such that few non-match pairs pass the High CMC criterion is critical to this method's success. An issue related to this is that there does not exist an agreed-upon set of alignment parameter thresholds nor a method, other than pure experimentation, by which these thresholds can be determined in the CMC literature.

Similar to the initially proposed method, the implementation in the **cmcR** package tends to give a larger number of false positive High CMCs to non-match pairs relative to results in the CMC literature. On the other hand, the number of CMCs assigned to matching pairs is comparable under both methods. Undoubtedly, finer tuning of the thresholding parameters would yield results more similar to those in the CMC literature. Additionally, further exploration of procedures by which the breech face impressions can be isolated and highlighted may help reduce the effects of characteristics of the scan that make it difficult to distinguish matches from non-matches. For example, cartridges from the same manufacturer may share similarities that cartridges from different manufacturers do not. Such similarities are often used by forensic practitioners to initially pare down the possible pool of matching cartridge cases ([Thompson, 2017](#)). However, not removing such characteristics might increase the probability of making a false positive matching identification.

Conclusion

The results shared in this manuscript indicate that the implementation of the CMC method in the **cmcR** package is at least qualitatively similar to those in the CMC literature. As such methods could potentially be used in the future as evidence to support legal conclusions, it is imperative that specific implementations be openly available for assessment and validation. Furthermore, reproducibility of results hinges on automating as much of the process by which these comparisons are made as possible. For example, selecting the region of a scan containing breech face impressions by hand, as is done in the CMC literature ([Song et al., 2018](#)), will yield different results depending on who is performing the

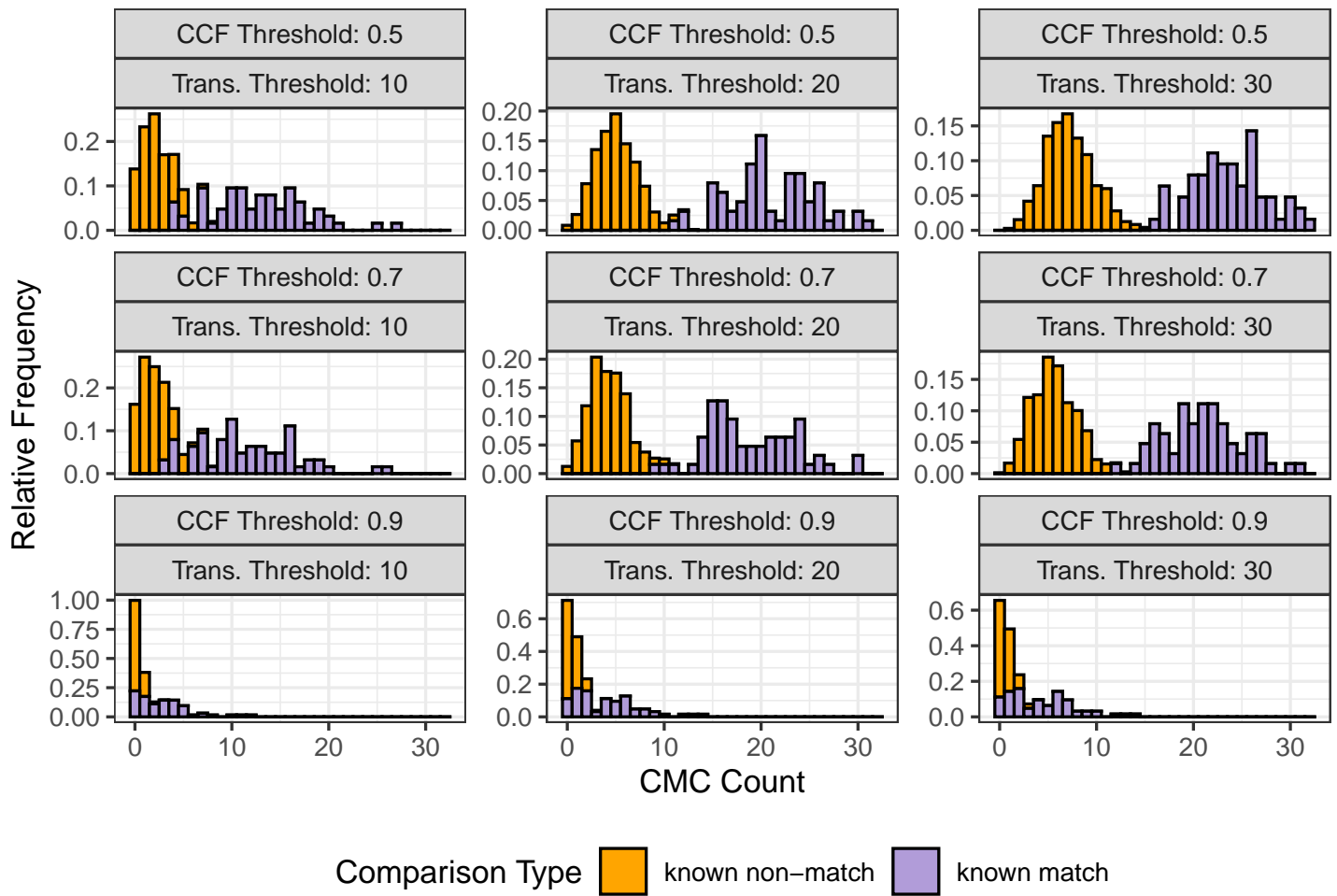


Figure 12: Initial CMC count distributions for various T_{dx} , T_{dy} , and T_{CCF} values and $T_\theta = 6$ degrees.

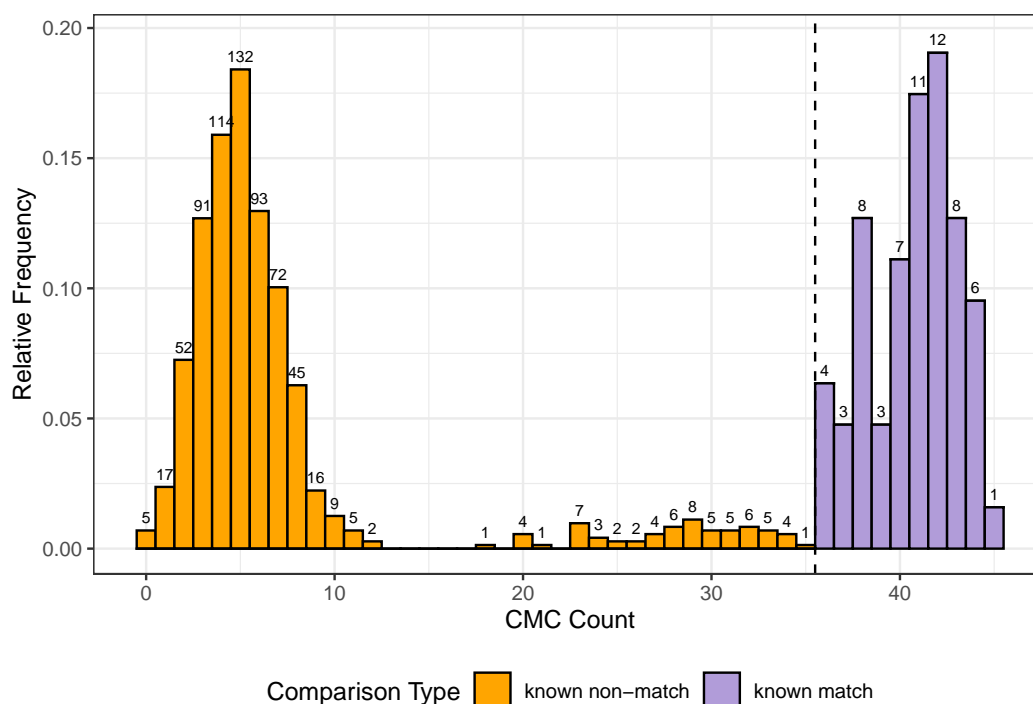


Figure 13: High CMC count distribution with $T_{CCF} = .5$, $T_{dx} = T_{dy} = 20$, and $T_{\theta} = 6$ degrees

selection. The procedure implemented in the **cmcR** package using the RANSAC and Hough transform methods, while reliant on randomly sampling the surface matrix, at least yields reproducibility across applications by setting a seed. Lastly, it is simply best academic practice to be transparent about how certain results were obtained and how sensitive these results are to different processing conditions. The **cmcR** package is intended to provide researchers with an automatic, transparent tool to further explore the potential of the CMC method and develop novel techniques to perform firearm evidence identification.

Future changes to the current implementation will likely come in the form of improvements to the way that breech face impressions are automatically isolated and highlighted within the scan. For example, a Robust Gaussian Regression Filter can be used to simultaneously isolate and filter the breech face impression region in the surface matrix (Muralikrishnan and Raja, 2008). There are also a number of other extensions to the initially proposed CMC method that currently lack an open-source implementation. The foundation set by the **cmcR** package should make it easier to implement these extensions in the future.

Bibliography

- E. O. Brigham. *The Fast Fourier Transform and Its Applications*. Prentice-Hall, Inc., USA, 1988. ISBN 0133075052. [p3]
- Z. Chen, J. Song, W. Chu, J. A. Soons, and X. Zhao. A convergence algorithm for correlation of breech face images based on the congruent matching cells (CMC) method. *Forensic Science International*, 280: 213–223, Nov. 2017. ISSN 03790738. doi: 10.1016/j.forsciint.2017.08.033. URL <https://linkinghub.elsevier.com/retrieve/pii/S0379073817303420>. [p2, 5, 10, 11]
- T. Fadul, G. Hernandez, S. Stoiloff, and G. Sneh. An Empirical Study to Improve the Scientific Foundation of Forensic Firearm and Tool Mark Identification Utilizing 10 Consecutively Manufactured Slides, 2011. [p2, 5, 7, 10]
- M. A. Fischler and R. C. Bolles. Random sample consensus: A paradigm for model fitting with applications to image analysis and automated cartography. *Commun. ACM*, 24(6):381–395, June 1981. ISSN 0001-0782. doi: 10.1145/358669.358692. URL <https://doi.org/10.1145/358669.358692>. [p7]
- H. Hofmann, S. Vanderplas, G. Krishnan, and E. Hare. *x3ptools: Tools for Working with 3D Surface Measurements*, 2019. URL <https://github.com/heike/x3ptools>. R package version 0.0.2.9000. [p2]

High CMC counts for various CCF & translation thresholds, $T_\theta = 6^\circ$

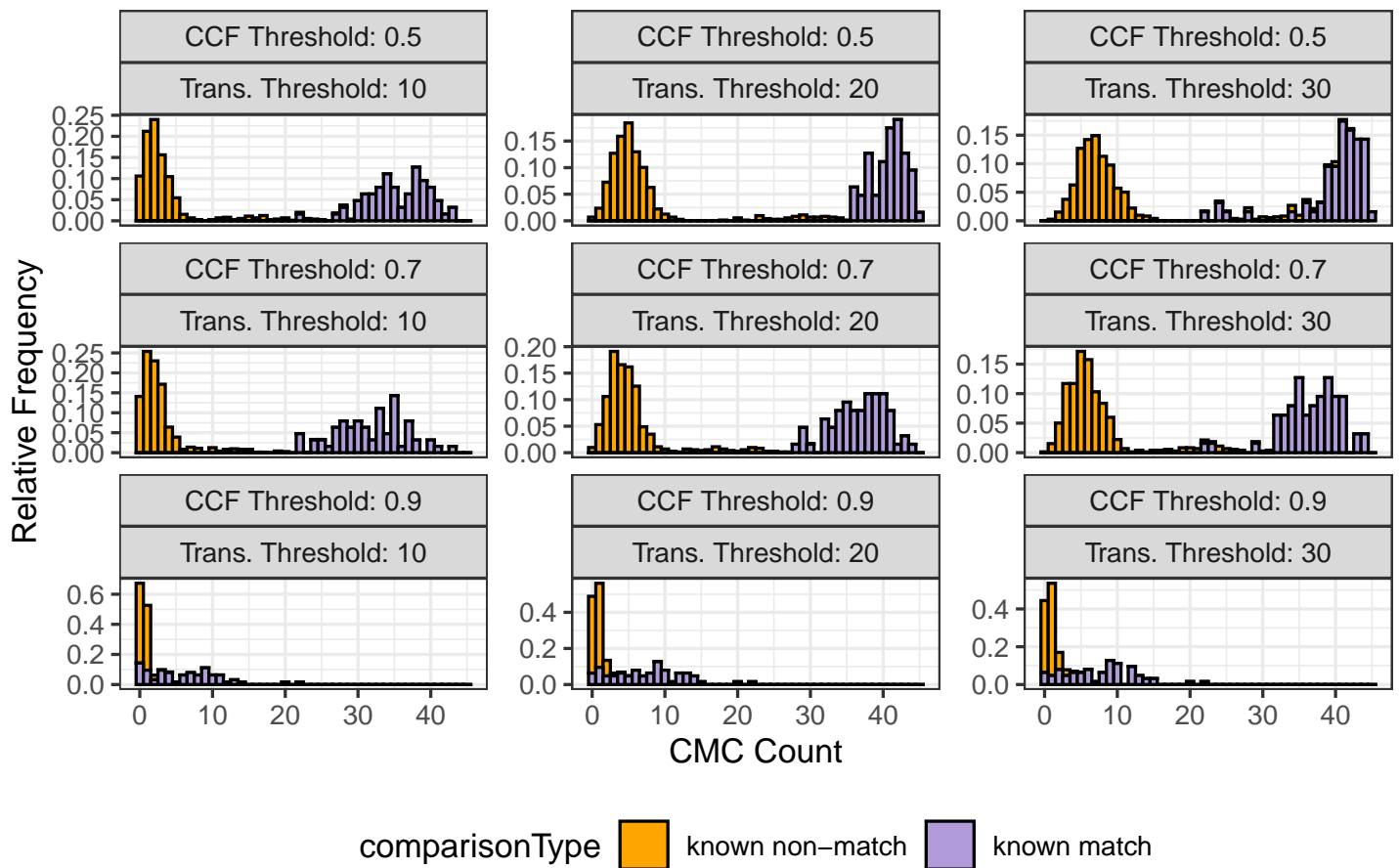


Figure 14: High CMC count distributions for various T_{dx} , T_{dy} , and T_{CCF} values and $T_\theta = 6$ degrees.

- P. Hough. Method and means for recognizing complex patterns, 1962. [p7]
- D. La Porte. An empirical validation study of breechface marks on .380 acp caliber cartridge cases fired from ten consecutively finished hi-point model c9 pistols. *AFTE Journal*, 43(4): 303–309, 2011. URL <https://tsapps.nist.gov/NRBTD/Studies/Studies/Details/4908a64a-702c-4203-a945-6279df3acf3f>. [p11]
- Michigan State Police. *Cartridge Case Identification*. 2020. URL michigan.gov/msp/0,4643,7-123-1564-15966--,00.html. [p1]
- B. Muralikrishnan and J. Raja. *Computational Surface and Roundness Metrology*. Springer Publishing Company, Incorporated, 1st edition, 2008. ISBN 1848002963. [p13]
- National Research Council. *Strengthening Forensic Science in the United States: A Path Forward*. The National Academies Press, Washington, DC, 2009. ISBN 978-0-309-13130-8. doi: 10.17226/12589. URL <https://www.nap.edu/catalog/12589/strengthening-forensic-science-in-the-united-states-a-path-forward>. [p1]
- D. Ott, R. Thompson, and J. Song. Applying 3D measurements and computer matching algorithms to two firearm examination proficiency tests. *Forensic Science International*, 271:98–106, Feb. 2017. ISSN 03790738. doi: 10.1016/j.forsciint.2016.12.014. URL <https://linkinghub.elsevier.com/retrieve/pii/S0379073816305461>. [p3]
- J. Song. Proposed “NIST Ballistics Identification System (NBIS)” Based on 3D Topography Measurements on Correlation Cells. *American Firearm and Tool Mark Examiners Journal*, 45(2):11, 2013. [p1, 2, 5, 10]
- J. Song, T. V. Vorburger, W. Chu, J. Yen, J. A. Soons, D. B. Ott, and N. F. Zhang. Estimating error rates for firearm evidence identifications in forensic science. *Forensic Science International*, 284:15–32, Mar. 2018. ISSN 03790738. doi: 10.1016/j.forsciint.2017.12.013. URL <https://linkinghub.elsevier.com/retrieve/pii/S0379073817305200>. [p1, 8, 10, 11]
- X. H. Tai and W. F. Eddy. A Fully Automatic Method for Comparing Cartridge Case Images,. *Journal of Forensic Sciences*, 63(2):440–448, Mar. 2018. ISSN 00221198. doi: 10.1111/1556-4029.13577. URL <http://doi.wiley.com/10.1111/1556-4029.13577>. [p7]
- R. Thompson. Firearm identification in the forensic science laboratory, 08 2017. [p1, 11]
- M. Tong, J. Song, and W. Chu. An Improved Algorithm of Congruent Matching Cells (CMC) Method for Firearm Evidence Identifications. *Journal of Research of the National Institute of Standards and Technology*, 120:102, Apr. 2015. ISSN 2165-7254. doi: 10.6028/jres.120.008. URL <https://nvlpubs.nist.gov/nistpubs/jres/120/jres.120.008.pdf>. [p2, 5, 6, 10]
- X. A. Zheng, J. A. Soons, and R. M. Thompson. Nist ballistics toolmark research database, 2016. [p2]

Joseph Zemmels
Iowa State University
2438 Osborn Dr
Ames, IA 50011
jzemmels@iastate.edu

Heike Hofmann
Iowa State University
2438 Osborn Dr
Ames, IA 50011
hofmann@iastate.edu

Susan VanderPlas
University of Nebraska - Lincoln
340 Hardin Hall North Wing
Lincoln, NE 68583
susan.vanderplas@unl.edu